

Positive- and Negative-Pulsed Streamer Discharges Generated by a 100-ns Pulsed-Power in Atmospheric Air

Douyan Wang, Manabu Jikuya, Seishi Yoshida, Takao Namihira, *Senior Member, IEEE*, Sunao Katsuki, *Member, IEEE*, and Hidenori Akiyama, *Fellow, IEEE*

Abstract—A Blumlein generator that has a pulsewidth of 100 ns was used to investigate the process of streamer discharge propagation in a coaxial cylindrical reactor using a streak camera. Both positive and negative polarities of the streamer discharges were performed in air at atmospheric pressure. The results showed that the primary and secondary streamers propagated with increasing velocity from the central rod to the outer cylinder electrode in both positive and negative polarities of applied voltages to the rod electrode. The propagation velocity of the streamer heads was in the range of 0.8–1.2 mm/ns for a positive peak applied voltage in the range of 43–60 kV and 0.6 mm/ns for a negative peak applied voltage of –93 kV, respectively. The electric field at streamer onset was calculated to be 12 and 20 MV/m for positive and negative applied voltages, respectively.

Index Terms—Atmospheric pressure air, coaxial electrode, electric field, nanosecond pulse, propagation velocity, pulsed streamer discharge, streamer onset.

I. INTRODUCTION

NONTHERMAL plasmas have been one of the promising technologies for the removal of hazardous environmental pollutants in gases. A pulsed streamer discharge in atmospheric pressure gases is one type of nonthermal plasma and has received a great deal of interest for many years [1]. The critical factor to enable this technique for industrial application of pollutant removal is to improve the energy efficiency of the plasma processing. It is already known that the pulsewidth of the applied voltage has a strong influence on obtaining higher energy efficiency [2], [3]. For further investigations, it is necessary to know the propagation mechanism of the pulsed streamer discharges.

During the past few decades, many numerical and experimental studies on positive streamer discharges (cathode directed streamer) have been reported [4]–[10]. In addition, a small number of analysis on negative pulsed streamer discharges (anode directed streamer) have been carried out [7], [10]. Wagner investigated the development of both positive and negative streamers by means of image intensification and image deflection to determine the conditions for streamer onset and streamer velocities during the various stages of the

avalanche-to-plasma channel transition in several gases in the pressure range of 100–500 torr. The enhanced and accelerated streamer stage was observed in both directions; the significantly fast and steep ionization waves were found to start at the cathode as well as at the anode on arrival of the respective streamers. The measured velocities were up to 10 mm/ns [8], [9].

In addition, the emission from positive pulsed streamer discharges in air at atmospheric pressure was observed with an intensified charge-coupled device camera with a high-speed gate in previous work in which the streamer propagation process and its propagation velocity in a coaxial electrode were reported [11]. In this paper, the detailed propagation characteristics of a pulsed streamer discharge produced by both positive and negative voltages in a coaxial electrode filled with atmospheric pressure air are reported. The pulsewidth of the applied voltage was fixed at 100 ns. The propagation process and velocity of the streamer obtained by a high-dynamic-range streak camera is reported under different applied voltages, and the electric field for streamer onset is also investigated.

II. EXPERIMENTAL APPARATUS AND PROCEDURE

Fig. 1 shows a schematic diagram of the experimental apparatus used to observe the positive and negative pulsed streamer discharges. A three-staged Blumlein line generator with a pulsewidth of 100 ns was used as a pulsed-power supply in this paper [11]. For generation of positive polarity pulse voltages, this generator was charged to 20, 25, and 30 kV by a dc high voltage source (LT50R35; Glassman High Voltage, Inc., High Bridge, NJ). Negative pulsed voltages were generated when this generator was charged to –20, –25, and –30 kV. To reduce switching jitter, a thyatron switch (CX1685; E2V Technologies, Ltd., Chelmsford, U.K.) with smaller jitter than spark gap switches was employed as a closing switch for the Blumlein line generator. A coaxial cylindrical reactor was utilized as a discharge electrode to observe pulsed streamer discharges. A rod made of stainless steel that is 0.5 mm in diameter and 10 mm in length was placed concentrically in a copper cylinder. The outer cylinder wall electrode was grounded, and its diameter was 76 mm. A short length of the electrodes was necessary to render clear images of the streamer discharge. Dry air at 0.1 MPa filled the reactor volume. For each test, a positive or negative polarity voltage from the Blumlein line generator was applied to the rod electrode and was measured using a voltage divider (EP-100K;

Manuscript received September 26, 2005; revised June 4, 2007.

The authors are with the Department of Electrical and Computer Engineering, Kumamoto University, Kumamoto 860-8555, Japan (e-mail: namihira@es.kumamoto-u.ac.jp).

Digital Object Identifier 10.1109/TPS.2007.902132

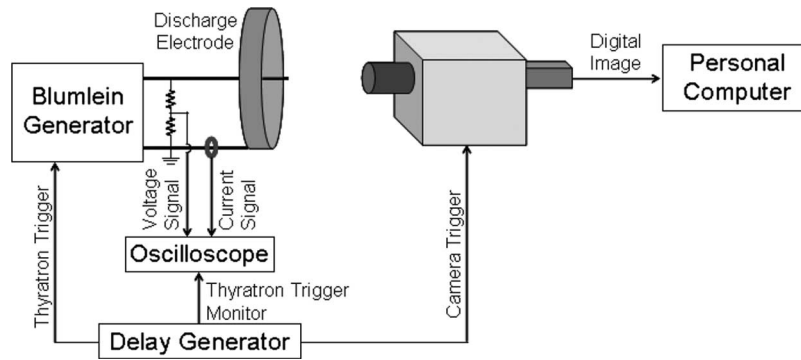


Fig. 1. Schematic diagram of the experimental apparatus.

Pulse Electronic Engineering Co., Ltd., Noda, Japan). The discharge current through the electrodes was measured using a current transformer (Pearson current monitor; Model 2878; Pearson Electronics Inc., Palo Alto, CA), which was located on the return current path to the ground. A digital oscilloscope (54855A Infiniium; Agilent Technologies, Santa Clara, CA) with a maximum bandwidth of 6 GHz and a maximum sample rate of 20 gigasample/s recorded the signals from the voltage divider and the current monitor. A fast-dynamic-range streak camera (C7700; Hamamatsu Photonics, Hamamatsu, Japan) with a sensitive microchannel plate (with a maximum gain of 10 000) was used to observe the streamer discharge propagation in the coaxial electrode. The sweep time for one frame of exposure was fixed at 200 ns. The slit of the streak camera was adjusted to focus on the central part of the discharge electrode, where the rod electrode was fixed at the center of streak image. The width of the camera slit was fixed at 50 μm . A digital delay generator (DG535; Stanford Research Systems, Inc., Sunnyvale, CA) controlled the trigger signals for the oscilloscope, thyatron, and streak camera. In this paper, only a single pulse was applied to the discharge electrode to observe the streamer image.

III. RESULT AND DISCUSSION

Fig. 2 shows the typical applied voltage and discharge current in the electrode gap, and the streak image at 30-kV dc charging voltage to the generator for positive streamer discharge propagation. In Fig. 2, the vertical direction of the streak image corresponds to the position within the electrode gap. The top and bottom ends of the streak image are the surfaces of the grounded cylinder and the central rod, respectively. The horizontal direction indicates time progression and the time scale of the voltage and current waveforms. It should be noted that the left part of the streak image, for time less than 0 ns, was cut short for better viewing. Fig. 3 shows a typical still photograph of a pulsed streamer discharge in the coaxial electrode. From Fig. 2 and our previous works [11], it can be confirmed that the streamer discharge propagates straight in the radial direction from the coaxial electrode. This is because the interactions between the electric fields of the neighboring streamer heads are the same within the coaxial electrode geometry [12], [13]. The streak images taken in this paper show the tracks of a single streamer head. In addition, the streak images had good

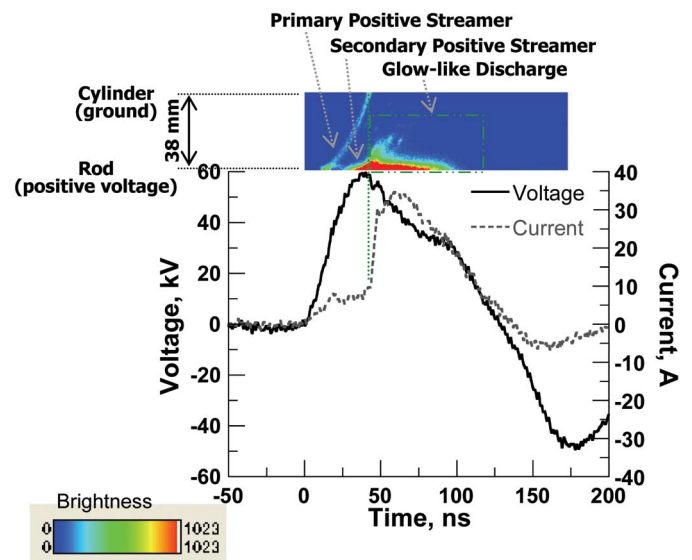


Fig. 2. Typical applied voltage and discharge current in the electrode gap, and streak image at 30-kV harging voltage for the generator (positive streamer discharge).

reproducibility under similar experimental conditions. Observe in Fig. 2 that the streamer initiates in the vicinity of the central rod electrode and then propagates toward the cylinder electrode (primary positive streamer, PPS) as the first step of the streamer discharge. The PPS track was recorded as a line shape. This is because the high electric field generated around the streamer head results from the surrounding positive charges; therefore, only the streamer head is bright during the propagation of PPS [14]–[20]. In addition, the propagation velocity of the PPS increases with its propagation. After the PPS left the rod electrode, a second streamer was generated in the vicinity of the rod electrode (secondary positive streamer, SPS). This may be due to the electric field on the surface of wire electrode recovering enough to generate another streamer discharge along the propagation path of the PPS. After generation, the SPS propagated toward the cylinder electrode with a lower velocity than PPS. This is because the SPS propagates in the plasma channel produced by the PPS propagation, and it means that the electric field near the SPS head is lower than that of the PPS. At the time of full development of the PPS between the electrodes (time at the peak applied voltage), the SPS disappeared at the middle of the electrode gap, and the discharge mode changed from streamer to glowlike discharges

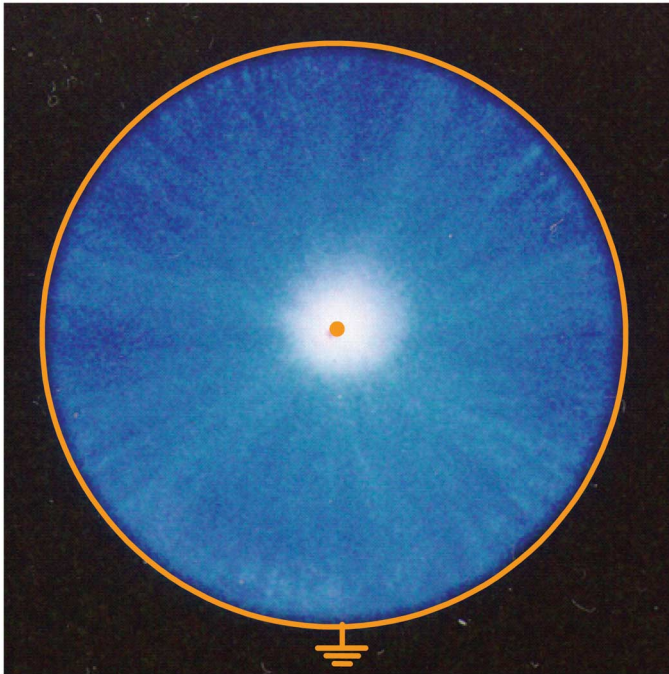


Fig. 3. Typical still image of a pulsed streamer discharge taken from the axial direction in the coaxial electrode.

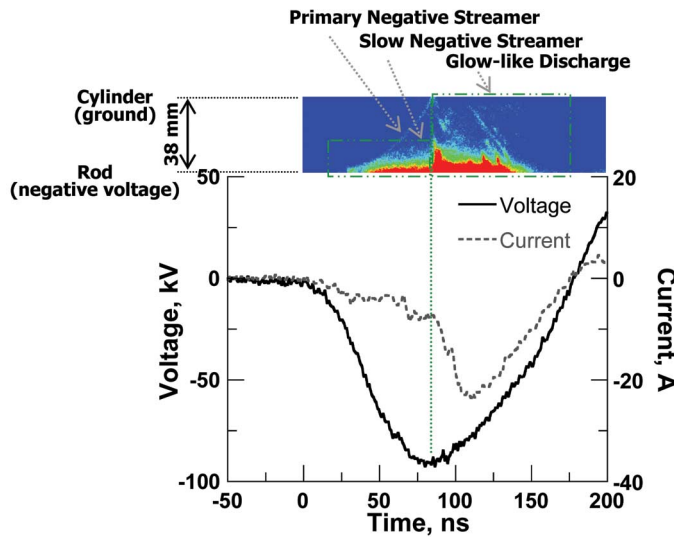


Fig. 4. Typical applied voltage and discharge current in the electrode gap, and streak image at -30-kV charging voltage for the generator (negative streamer discharge).

with a large flow of current in the plasma channel produced by the PPS propagation. Similar phenomena were observed for 20- and 25-kV dc charging voltages.

Fig. 4 shows the typical applied voltage and discharge current in the electrode gap and a streak image for a negative streamer discharge at -30-kV dc charging voltage to the generator. Observe in Fig. 4 that the primary negative streamer (PNS = fast negative streamer) initiates in the vicinity of the central rod electrode and then propagates toward the cylinder wall electrode. The discharge emission of the slow negative streamer (SNS) was recorded near the surface of the rod electrode. It is believed that the streamer head of the PNS propagates faster due

TABLE I
AVERAGE VELOCITY OF PRIMARY STREAMER HEADS

Charging voltage		20 kV dc	25 kV dc	30 kV dc
Polarity				
Positive		0.8 mm/ns	1.0 mm/ns	1.2 mm/ns
	($V_{\text{applied-peak}}$)	(43 kV)	(56 kV)	(60 kV)
Negative		-	-	0.6 mm/ns
	($V_{\text{applied-peak}}$)	(-64 kV)	(-80 kV)	(-93 kV)

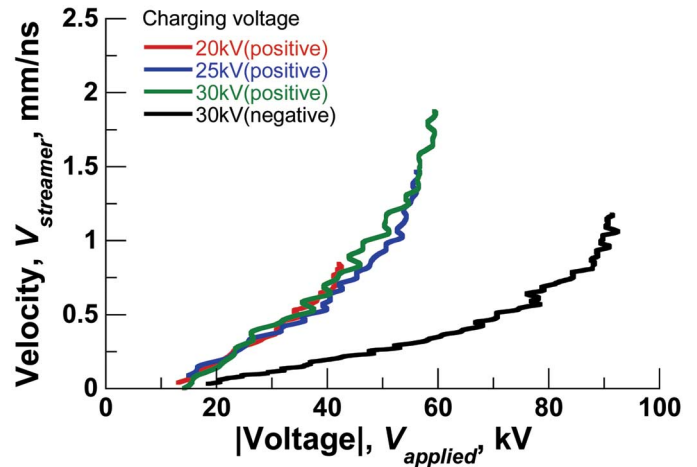


Fig. 5. Dependence of the velocity of the streamer heads on the applied voltage to the rod electrode for both positive and negative streamer discharge cases.

TABLE II
ELECTRIC FIELD FOR STREAMER ONSET

Polarity		Positive	Negative
Parameter		streamer	streamer
$V_{\text{applied-at streamer onset}}$		15 kV	-25 kV
E_{on}		12 MV/m	20 MV/m

to the surrounding photoionization, and then the heat of the rod electrode surface allows the SNS to propagate slower, following the PNS. After full development of the PNS across the electrode gap (time at the peak applied voltage), the discharge mode changed from a streamer to a glowlike discharge with a large discharge current, which is the same as the positive one. For the negative streamer discharge case, the development of the PNS was not observed for -20- and -25-kV dc charging voltages. This is because the applied electric field was insufficient for PNS onset.

Table I shows the average velocity of the primary streamer heads in the experiment. The average velocity is calculated as the gap distance divided by the time from initiation of the streamer head on the rod electrode to its arrival at the cylinder electrode. The average propagation velocity of the positive streamers was in the range of 0.8–1.2 mm/ns for a positive peak applied voltage in the range of 43–60 kV. This result is

TABLE III
COMPARISON OF THE STREAMER VELOCITY AND ELECTRIC FIELD ON THE SURFACE OF THE HIGH-VOLTAGE ELECTRODE OF THE PRESENTED EXPERIMENTAL RESULTS WITH OTHER SIMULATION RESULTS

Reference	Polarity	Electrode geometry	Gas medium and pressure	Applied voltage	Primary streamer velocity	Electric field on the surface of the high-voltage electrode at streamer onset	Equation for calculation of the electric field on the surface of the high-voltage electrode
Presented work (experiment)	Positive & Negative	Coaxial cylindrical (gap=38 mm)	Air, atmospheric pressure	Fig. 5	~ 1.8 mm/ns (Positive) ~ 1.3 mm/ns (Negative)	12 MV/m (@positive) 20 MV/m (@negative)	Equation (2)
H. Raether [18] (experiment)	Cathode-directed streamer Anode-directed streamer	Point-to-plate (gap=20 mm)	Air, 275 Torr	-	~ 0.3 mm/ns (Cathode-directed) ~ 0.015 mm/ns (Anode-directed)	$E_{\max}/E_{\min} > 100$	-
Tochikubo <i>et al.</i> [21] (numerical simulation)	Positive	Point-to-plane (gap=10 mm)	Air/NO(300 ppm), atmospheric pressure	15 kV dc	0.6 mm/ns	23 MV/m	Equation (3)
Pancheshnyi <i>et al.</i> [22] (numerical simulation)	Cathode-directed streamer	Point-to-plane (gap=30 mm)	Air, atmospheric pressure	12 kV dc	0.4 mm/ns	79 MV/m	Equation (3)
Grange <i>et al.</i> [23] (numerical simulation)	Positive	Point-to-plane (gap=10 mm)	Air, atmospheric pressure	8 kV dc	0.2 mm/ns	27 MV/m	Equation (3)

in good agreement with our previous data calculated from other images of streamer discharge propagation [11]. On the other hand, the velocity for negative streamers was approximately half that of positive streamers. The same tendency was observed in the early study of Raether [18], shown in Table III.

Fig. 5 shows the dependence of the velocity of primary streamer heads on the applied voltage to the rod electrode in both cases of positive and negative voltage applications. The propagation velocity of the streamer heads at a certain time v_{streamer} is given by

$$v_{\text{streamer}} = \frac{\Delta L}{\Delta t} \quad (1)$$

where ΔL and Δt are the developed distance and time progress for its propagation from the streak images (Figs. 2 and 4), respectively. Observe in Fig. 5 that the velocity of PPS is the same at a certain applied voltage for different charging voltages, and the velocity increases with increasing applied voltage to the rod electrode. This may be due to the applied voltage to the rod electrode having a strong influence on the motion of the streamer head since there is a higher conductivity plasma channel between the rod and streamer head. For 60-kV applied voltage and 30-kV charging voltage, the velocity of the PPS reaches 1.9 mm/ns. The velocity of a PNS is approximately half that of positive streamers and also increases by increasing the absolute value of the applied voltage to the rod electrode. For -90 kV applied voltage, the velocity of the NPS reaches 1.2 mm/ns.

In this paper, it was also demonstrated that the electric field for PPS onset was constant at 15 kV for all different applied voltages in positive streamers. Likewise, the applied voltage at streamer onset was -25 kV for negative streamers. The electric field on the surface of the rod electrode before discharge initiation E_0 is given by

$$E_0 = \frac{|V_{\text{applied}}|}{r \ln \frac{r_2}{r_1}} \quad (2)$$

where $|V_{\text{applied}}|$, r , r_1 , and r_2 are the absolute value of the applied voltage to the rod electrode, the distance from the center of the rod electrode, the radius of the rod electrode, and the inner radius of the cylinder electrode, respectively. At the rod electrode surface, $r = r_1$. The electric field on the surface of the rod electrode at the streamer onset E_{on} can then be calculated by (2) and is indicated in Table II. From Table II, the positive and negative streamer onset fields were 12 and 20 MV/m, respectively.

Table III shows a comparison of the streamer velocities and electric fields on the surface of the high-voltage electrode for the presented experimental results and for other reported simulation results [21]–[23]. In Table III, the electric field at the tip of the high-voltage electrode in a point-to-plane electrode geometry E_p is given by

$$E_p = V \frac{2}{r} \left(\frac{d+r}{d} \right)^{1/2} \left/ \ln \frac{1 + \{d/(d+r)\}^{1/2}}{1 - \{d/(d+r)\}^{1/2}} \right. \quad (3)$$

where V , r , and d are the applied voltage, the radius of the tip of the electrode, and the gap length, respectively [24]. From Table III, it is obvious that the streamer velocity calculated by the numerical models is lower than the experimental results presented, although the electric fields for streamer onset were higher. This might be caused by the difference of the applied voltage. For modeling, a dc applied voltage was used, and a constant velocity was calculated. However, in this paper, a pulsed voltage was applied, and the streamer propagated with acceleration. The results in this paper, particularly, Fig. 5, give more information of the streamer velocity at different applied voltages, which would shed light on the utility of modeling the streamer propagations.

IV. CONCLUSION

Streamer propagation, streamer velocity, and the electric field for streamer onset were investigated for positive and negative applied pulsed voltages to the rod electrode of a coaxial electrode. Four conclusions have been deduced.

- 1) The head of the streamer discharge initiated at the surface of the central rod electrode and then propagated to the outer cylinder electrode for both positive and negative voltage cases.
- 2) The average propagation velocity of the streamer heads was in the range of 0.8–1.2 mm/ns for a positive peak applied voltage in the range of 43–60 kV. The velocity for PNS was 0.6 mm/ns for a negative peak voltage of –93 kV.
- 3) The velocity increased with increasing applied voltage to the rod for both positive and negative voltage cases.
- 4) The electric field at streamer onset was calculated as 12 and 20 MV/m for positive and negative streamers, respectively.

REFERENCES

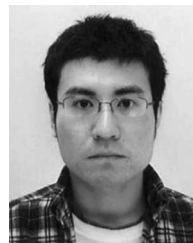
- [1] B. M. Penetrante, M. C. Hsiao, B. T. Merritt, G. E. Vogtlin, and P. H. Wallman, "Comparison of electrical discharge techniques for non-thermal plasma processing of NO and NO₂," *IEEE Trans. Plasma Sci.*, vol. 23, no. 4, pp. 679–687, Aug. 1995.
- [2] T. Namihira, S. Tsukamoto, D. Wang, S. Katsuki, R. Hackam, H. Akiyama, Y. Uchida, and M. Koike, "Improvement of NO_x removal efficiency using short width pulsed power," *IEEE Trans. Plasma Sci.*, vol. 28, no. 2, pp. 434–442, Apr. 2000.
- [3] V. Puchkarev and M. Gundersen, "Energy efficient plasma processing of gaseous emission using a short pulse discharge," *Appl. Phys. Lett.*, vol. 71, no. 23, pp. 3364–3366, Dec. 1997.
- [4] N. Y. Babaeva and G. V. Naidis, "Two-dimensional modeling of positive streamer propagation in flue gases in sphere-plane gaps," *IEEE Trans. Plasma Sci.*, vol. 26, no. 1, pp. 41–45, Feb. 1998.
- [5] A. A. Kulikovskiy, "Analytical model of positive streamer in weak field in air: Application to plasma chemical calculations," *IEEE Trans. Plasma Sci.*, vol. 26, no. 4, pp. 1339–1346, Aug. 1998.
- [6] R. Ono and T. Oda, "Nitrogen oxide γ -band emission from primary and secondary streamers in pulsed positive corona discharge," *J. Appl. Phys.*, vol. 97, no. 1, p. 013302, Jan. 2005.
- [7] E. H. W. M. Smulders, B. E. J. M. van Heesch, and S. S. V. B. van Passen, "Pulsed power corona discharges for air pollution control," *IEEE Trans. Plasma Sci.*, vol. 26, no. 5, pp. 1476–1484, Oct. 1998.
- [8] K. H. Wagner, "Die Entwicklung der Elektronenlawine in den Plasmakanal, untersucht mit Bildverstärker und Wischverschluss," *Zeitschrift für Physik*, vol. 189, no. 5, pp. 465–515, Oct. 1966.
- [9] K. H. Wagner, "Vorstadium des Funkens, untersucht mit dem Bildverstärker," *Zeitschrift für Physik*, vol. 204, no. 2, pp. 177–197, Feb. 1967.
- [10] P. P. M. Blom, "High-Power Pulsed Corona," Ph.D. dissertation, Technische Universiteit Eindhoven, Eindhoven, The Netherlands, 1997.
- [11] T. Namihira, D. Wang, S. Katsuki, R. Hackam, and H. Akiyama, "Propagation velocity of pulsed streamer discharges in atmospheric air," *IEEE Trans. Plasma Sci.*, vol. 31, no. 5, pp. 1091–1094, Oct. 2003.
- [12] D. Wang, T. Namihira, K. Fujiya, S. Katsuki, and H. Akiyama, "The reactor design for diesel exhaust control using a magnetic pulse compressor," *IEEE Trans. Plasma Sci.*, vol. 32, no. 5, pp. 2038–2044, Oct. 2004.
- [13] Y. H. Kim and S. H. Hong, "Two-dimensional simulation images of pulsed corona discharge in a wire-plate reactor," *IEEE Trans. Plasma Sci.*, vol. 30, no. 1, pp. 168–169, Feb. 2002.
- [14] L. B. Loeb, "Ionizing waves of potential gradient," *Science*, vol. 148, no. 3676, p. 1417, Jun. 1965.
- [15] L. B. Loeb, *Fundamental Processes of Electrical Discharges in Gases*. New York: Wiley, 1939.
- [16] J. M. Meek, "A theory of spark discharges," *Phys. Rev.*, vol. 57, no. 8, p. 722, Apr. 1940.
- [17] J. M. Meek and J. D. Craggs, *Electrical Breakdown of Gases*. Oxford, U.K.: Clarendon, 1953, pp. 251–290.
- [18] H. Raether, *Electron Avalanches and Breakdown in Gases*. London, U.K.: Butterworth, 1964.
- [19] E. Marode, "The mechanism of spark breakdown in air at atmospheric pressure between a positive point and a plane—Part I: Experimental: Nature of the streamer track," *J. Appl. Phys.*, vol. 46, no. 5, pp. 2005–2015, May 1975.
- [20] E. Marode, "The mechanism of spark breakdown in air at atmospheric pressure between a positive point and a plane—Part II: Computer simulation of the streamer track," *J. Appl. Phys.*, vol. 46, no. 5, pp. 2016–2020, May 1975.
- [21] F. Tochikubo and H. Arai, "Numerical simulation of streamer propagation and radical reactions in positive corona discharge in N₂/NO and N₂/O₂/NO," *Jpn. J. Appl. Phys.*, vol. 41, no. 2A, pp. 844–852, Feb. 2002.
- [22] S. Pancheshnyi, M. Nudnova, and A. Starikovskii, "Development of a cathode-directed streamer discharge in air at different pressures: Experiment and comparison with direct numerical simulation," *Phys. Rev. E, Stat. Phys. Plasmas Fluids Relat. Interdiscip. Top.*, vol. 71, no. 1, p. 016407, Jan. 2005.
- [23] F. Grange, N. Soulem, J. F. Loiseau, and N. Spyrou, "Numerical and experimental determination of ionizing front velocity in a DC point-to-plane corona discharge," *J. Phys. D, Appl. Phys.*, vol. 28, no. 8, pp. 1619–1629, 1995.
- [24] I. Ishii and T. Noguchi, "Dielectric breakdown of supercritical helium," *Proc. IEE*, vol. 126, no. 6, pp. 532–536, Jun. 1979.



Douyan Wang was born in Beijing, China, on May 18, 1975. She received the B.S., M.S., and Ph.D. degrees from Kumamoto University, Kumamoto, Japan, in 1998, 2000, and 2005, respectively. From 2000 to 2002, she was with Hitachi, Ltd., Ibaraki, Japan.

From 2003 to 2005, she was a JSPS Research Fellow. She is currently a Research Associate of the 21st Century Center of Excellence Program in the Department of Electrical and Computer Engineering, Kumamoto University.

Dr. Wang was the recipient of the Excellent Student Award of the IEEE Fukuoka Section in 2005.



Manabu Jikuya was born in Kagoshima, Japan, on November 13, 1981. He received the B.S. and M.S. degrees from Kumamoto University, Kumamoto, Japan, in 2004 and 2006, respectively.

Since 2006, he has been with Micarome Industrial Co., Ltd., Isahaya, Japan.



Seishi Yoshida was born in Kumamoto, Japan, on September 26, 1981. He received the B.S. and M.S. degrees from Kumamoto University, Kumamoto, Japan, in 2004 and 2006, respectively.

Since 2006, he has been with Aishin Seiki Co., Ltd., Kariya, Japan.



Sunao Katsuki (M'99) was born in Kumamoto, Japan, on January 5, 1966. He received the B.S., M.S., and Ph.D. degrees from Kumamoto University, Kumamoto, Japan, in 1989, 1991, and 1998, respectively.

He is currently with Kumamoto University, where he was a Research Associate from 1991 to 1998 and an Associate Professor from 1998 to 2007, and has been a Professor in the Department of Electrical and Computer Engineering since 2007.



Takao Namihira (M'00–SM'05) was born in Shizuoka, Japan, on January 23, 1975. He received the B.S., M.S., and Ph.D. degrees from Kumamoto University, Kumamoto, Japan, in 1997, 1999, and 2003, respectively.

From 1999 to 2006, he was a Research Associate at Kumamoto University, where he is currently an Associate Professor in the Department of Electrical and Computer Engineering. During 2003–2004, he was on sabbatical leave at the Center for Pulsed-Power and Power Electronics, Texas Tech University, Lubbock.



Hidenori Akiyama (M'87–SM'99–F'00) received the Ph.D. degree from Nagoya University, Nagoya, Japan, in 1979.

From 1979 to 1985, he was a Research Associate at Nagoya University. In 1985, he joined the faculty in the Department of Electrical and Computer Engineering, Kumamoto University, Kumamoto, Japan, where he is currently a Professor.

Prof. Akiyama was the recipient of the IEEE Major Education Innovation Award in 2000 and the IEEE Peter Haas Award in 2003.